LATENT AND SENSIBLE ENERGY FLUX OVER DEFORESTED LAND SURFACES IN THE EASTERN AMAZON AND NORTHERN THAILAND

T.W. Giambelluca[1], M.A. Nullet[1], A.D. Ziegler[1] and L. Tran[2]
[1]Department of Geography, University of Hawai'i at Manoa, Honolulu, USA
[2]Center for Integrated Regional Assessment, The Pennsylvania State University, Pennsylvania, USA

ABSTRACT

Land cover change may impact watershed hydrology and regional climate by altering land-atmosphere exchanges of energy and water. Conversion of forest to pasture has previously been shown to decrease the rate of evaporation (including transpiration) because of reduced aerodynamic roughness, less canopy rainfall interception and greater canopy resistance during dry periods. However, less is known about the effects of forest replacement land covers other than pasture. In this study, field measurements of meteorological processes, stomatal resistance, and Leaf Area Index (LAI) were taken over various deforested land surfaces in the eastern Amazon Basin and in northern Thailand. Based on these measurements, evaporation and sensible heat flux were estimated over each site. Results show the degree to which different land covers replacing tropical forest affect energy partitioning. In comparison with forest, non-irrigated, actively and recently cultivated sites had sharply lower rates of evaporation. Secondary vegetation generally had higher rates of evaporation than actively or recently used sites. The proportion of energy used for evaporation increased rapidly with age in secondary vegetation. Evaporation rates at sites eight and 25 years after abandonment in the Thailand study area were enhanced by positive sensible energy advection from nearby cultivated areas, and were similar to those of primary forest. Differences in dry season evaporation rates of 3-, 8- and 25-year secondary vegetation are explained, in part, by the differences in canopy resistance. Minimum canopy resistance was 223, 61 and 58 s m^{-1}, respectively at the 3-, 8 - and 25-year sites.

INTRODUCTION

Land cover change affects energy and mass flows between the land surface and the atmosphere. Local and regional climatic and hydrologic change may, therefore, result from land cover change. Decades of empirical watershed experiments and recent process studies and physically-based modeling efforts suggest a range of different hydrologic responses to reduction or replacement of forest cover in a basin (see Bruijnzeel, 1990; forthcoming). While advances have been made in understanding the atmospheric and hydrologic effects of land cover change, questions remain regarding the different influences of the various types of land cover replacing forest.

Singapore Journal of Tropical Geography, 21(2), 2000, 107-130

Deforestation alters the disposition of radiant energy by increasing surface albedo and daytime long-wave emission by the surface, resulting in lower net radiation (e.g. Bastable *et al*., 1993; Culf *et al*., 1995; Giambelluca *et al*., 1997; 1999). Net radiation is partitioned primarily into latent energy flux (evaporation and transpiration) and sensible energy flux (heating of the lower atmosphere). The characteristics and variable state of the land surface control this partitioning process. Moist, rough surfaces generally convert a large portion of net radiation into latent energy flux. Replacing forest with other land covers may change the proportions of energy going into latent and sensible flux because of differences in leaf area, aerodynamic roughness, root depth and stomatal behaviour. During and immediately following rainfall, evaporation of intercepted water is the dominant process. Reduction in canopy water storage capacity and air turbulence near the surface therefore result in lower rates of wet-canopy evaporation following deforestation. For periods when the canopy is dry, most observations indicate that transpiration is higher for forests than replacement land covers, because of greater turbulence generated over tall vegetation, higher leaf area of forests, and deeper root penetration of large trees. Field studies by Jipp *et al*. (1998) and Wright *et al*. (1992) found significantly lower latent energy flux over pasture than over forest in the Amazon. Because conversion of forest to pasture or grassland reduces evaporation[1], streamflow generally increases, possibly increasing flood hazard. However, throughout the tropics, a variety of land covers other than pasture are found in former forested areas. As Bruijnzeel (forthcoming) emphasizes, the effects of deforestation on evaporation and streamflow are not uniform, and depend on the original forest type, characteristics of replacement land cover, climate, exposure and soil depth.

[1]Except where otherwise specified, "evaporation" in this paper is equivalent to "evapotranspiration".

In addition to local effects described above, land-atmosphere feedbacks may lead to regional changes in rainfall. As much as 25 to 56 per cent of Amazon Basin rainfall is estimated to be derived from "recycling" of water evaporated within the basin (Eltahir & Bras, 1996). Basin rainfall, therefore, may decrease if evaporation is reduced by deforestation. A series of General Circulation Model (GCM) simulations (e.g. Nobre *et al*., 1991; Polcher & Laval, 1994; McGuffie *et al*., 1995; Henderson-Sellers *et al*., 1996; Xue *et al*., 1996) suggests that replacement of the entire Amazon rainforest with pasture could reduce evaporation and alter atmospheric circulation, decreasing basin rainfall by as much as 20 per cent.

While conversion of large tracts of tropical forest to grassland may produce significant local and regional impacts on energy and water fluxes, the consequences of more realistic scenarios of future land cover change in the tropics are less certain. It is reasonable to predict that a future deforested tropical landscape will not be solely grassland or degraded pasture but, instead, will be composed of a variety of replacement land covers. For example, much of the existing deforested areas of the Amazon and Thailand are covered with secondary vegetation at different stages of succession (Moran *et al*., 1994; Fox *et al*., 1995). The degree to which large-scale hydrologic processes will be affected by tropical deforestation depends on the physical characteristics, size and shape of spatial units composing the land-cover mosaic that will replace forest. Much of the uncertainty in current predictions of deforestation effects stems from a lack of information about the behaviour of various replacement land covers and possible interaction among different land cover patches in a highly fragmented landscape. Prior field studies (e.g. Wright *et al*., 1992; Bastable *et al*., 1993) have improved understanding of energy fluxes over pasture. However, relatively few observations have been made over other replacement land covers, such as secondary vegetation.

We have previously presented estimates of the physical characteristics of vegetation and soils for a variety of deforested sites, including secondary vegetation of different ages, in a small eastern Amazonian farm area and near a mountain village in northern Thailand (Giambelluca, 1996; Giambelluca *et al*., 1997; 1999). In general, we found that the characteristics of most deforested surfaces differed from forest, but less so than those of the extreme scenarios used in most GCM deforestation simulations (i.e. degraded pasture). In this paper, we present energy flux estimates based on field observations at those same sites. We attempt to show how the various land covers differ in the way they partition net radiation into sensible and latent heat flux. In particular, we look for evidence of reduced evaporative flux from recently cleared or actively cultivated sites and for any trend in energy partitioning as secondary vegetation matures. Our objective is to demonstrate the variability in land-atmosphere fluxes associated with the diverse land cover mosaic replacing forest.

METHODOLOGY

Field sites at Igarapé-Açu (Brazil) and Pang Khum (Thailand)

The Amazon Basin and Southeast Asia are two regions of major concern regarding the possible consequences of large scale tropical deforestation. The regions are physically and culturally distinct. The climate of peninsular Southeast Asia is strongly influenced by the adjacent ocean and modulated by the monsoon cycle and, therefore, less susceptible to land-cover-change-induced atmospheric feedbacks than the more continental Amazon region (Henderson-Sellers *et al*., 1996). Forest cover in the Amazon, though decreasing at an alarming rate, is much more extensive than that of Southeast Asia, where very little "old forest" remains. The cultural incentives and typical forest replacement land covers also differ between the two regions. The lure of cattle ranching remains a strong inducement to clear forest in South America. In the remaining forested areas of Southeast Asia, shifting cultivation is often identified as an important cause of deforestation, and cattle ranching is not extensive. The two study areas, Igarapé-Açu, Pará State, Brazil and Pang Khum, Chiang Mai Province, Thailand, are representative of these two contrasting regions. Agricultural practices at the two sites have in common the use of fire to prepare fields for cultivation, but differ in terms of crop preferences, length of fallow and use of irrigation.

Igarapé-Açu, Pará, Brazil is located in a lowland equatorial rainforest region (Sá *et al*, 1993). Agricultural practices in the village of Igarapé-Açu are typical of those of small farms in the deforested areas of the eastern Amazon Basin. Beginning in the early part of this century, the tropical rainforest in areas surrounding Igarapé-Açu has been replaced by secondary vegetation, areas cleared in preparation for planting field crops or pasture grass. Secondary vegetation, known locally as *capoeira*, grows during multi-year fallow periods in the traditional slash-and-burn cropping system of the region (Sá *et al*., 1993). Cassava, corn, cowpea and rice are the main crops (Kato & Denich, 1993). The equatorial climate of the region is characterized by a small annual cycle of temperature averaging 26ºC. About 2,500 mm of rainfall is received annually, with the highest amounts during February through April and the minimum during September through November (Bastos *et al.*, 1993). Soils at the site are ultisols, with loamy sand texture in the topsoil and sandy clay loam texture in the subsoil (Hölscher *et al*., 1997).

Pang Khum is a village located at an altitude of 1,250 m, north of Chiang Mai in northern Thailand. The site is in mountainous terrain with a monsoonal climatic regime and natural vegetation of lower montane forest (Hansen, 1992). It was originally settled 200 years ago by the Karen ethnic hilltribe group. During the past 20 years, members of Lisu ethnic group have settled in the village. The villagers of both groups practice swidden agriculture

on the slopes surrounding the settlement (Fox *et al.*, 1994). Paddy rice is also grown on terraced fields in the valley bottoms. Swidden crops, which were chiefly for subsistence in the past, now include vegetables, fruit, barley and cut flowers for sale outside the village. The population of the village (approximately 16 people km^{-1}) as well as the surrounding region is growing rapidly (Fox *et al.*, 1995). The increased land pressure has reduced fallow periods and expanded the area of cultivation at the expense of old growth forest. Rainfall has a well defined annual cycle. The rainy season extends from mid-May through October, during which approximately 90 per cent annual rainfall occurs. Mean annual rainfall at the site is approximately 1,100 to 1,300 mm. Mid-November through late February is the cool season, with mean air temperatures of around 17ºC. During the hot season, March to mid-May, air temperature averages about 25ºC, reaching daytime highs above 30ºC.

Instrumentation and measurements

Meteorological measurements were taken in both Igarapé-Açu and Pang Khum using a single set of sensors that was moved from site to site to produce a sequence of observations for different covers. Data were automatically sampled at 5-second intervals and averages were recorded every 10 minutes. Measurement periods varied from two to 37 days (Table 1). At each site, we measured solar radiation, reflected shortwave radiation, net radiation, soil heat conduction, canopy temperature (soil surface temperature in the case of bare soil), air temperature, humidity and rainfall. Instrumentation and data recording equipment are listed in Table 2. Soil heat conduction was measured with a heat flux plate inserted into the soil in a horizontal position, as close to the soil surface as possible without exposing the sensor to radiation (typically about 2 to 3 cm below the surface). We measured soil heat flux at only one point at each site, and we did not correct for changes in stored heat in the soil above the sensor. Canopy temperature was measured remotely using an infrared thermometer mounted above the canopy or bare soil surface. At Pang Khum, wind was measured at one or more height at each site and temperature and humidity were measured at more than one height at some sites. The Igarapé-Açu field site coincides with the SHIFT Project study area (Hölscher *et al*., 1997). The SHIFT meteorological tower was equipped with temperature and humidity profiling and radiation flux sensors for estimating evaporation via the Bowen ratio method. The tower also included an anemometer measuring wind velocity at 3.2 m above the ground. We added anemometers at 2.3 m and 6.8 m to the SHIFT meteorological tower to allow analysis of the vertical wind profile. Wind velocity at each of our Igarapé-Açu sites was estimated by adjusting measurements taken at the SHIFT tower to a reference height above the canopy or bare soil surface at each site. We argue that extrapolating the wind measurements in this manner is justified in this case because of the flat terrain and close proximity of the observation sites (all within 400 m of the SHIFT tower). Radiation, temperature and humidity sensor calibrations were adjusted on the basis of several in-field comparison runs.

In addition to continuous recording of meteorological observations, we operated a hand-held porometer to sample stomatal resistance and a ceptometer to measure canopy light interception at the sites with 3-, 8- and 25-year secondary vegetation (i.e. Sites (p), (q) and (r) respectively in Pang Khum). Photosynthetically active radiation (PAR) measurements were taken simultaneously with the ceptometer placed on or above the ground under the canopy and with a quantum sensor mounted above the canopy. Further explanation of the field observation methods can be found in earlier works (Giambelluca, 1996; Giambelluca *et al*., 1996; 1997; 1999).

Observations were taken primarily during the driest part of the year at each site (October and November 1992 in Igarapé-Açu and January through May 1993 in Pang Khum). At Pang Khum measurements continued into

TABLE 1. OBSERVATION PERIODS FOR FIELD MEASUREMENT SITES IN BRAZIL AND THAILAND

SITE	LENGTH OF OBSERVATION (days)	MEASUREMENT PERIOD
Igarapé-Açu, Brazil		1992
(a) Slashed vegetation	8	7-14 October
(b) Burned slash	2	5-7 November
(c) Bare soil	2	7-9 November
(d) Mature cassava	2	14-16 October
(e) Unused pasture	2	28-30 October
(f) ½ yr Secondary vegetation	2	21-23 October
(g) 1-yr Secondary vegetation	2	16-19 October
(h) 1-yr Secondary vegetation	3	19-21October
(i) 2-yr Secondary vegetation	3	23-26 October
(j) 2-yr Secondary vegetation	2	26-28 October
(k) 10-yr Secondary vegetation	5	30 October-5 November
Pang Khum, Thailand		1993
(l) Harvested barley	8	13-21 March
(m) Fallow rice paddy	15	26 April-11 May
(n) Irrigated bare soil	6	24-30 March
(o) 2-yr Secondary vegetation	6	7-13 March
(p) 3-yr Secondary vegetation	9	30 March-8 April
(q) 8-yr Secondary vegetation	37	24 January-2 March
(r) 25-yr Secondary vegetation	25	9-21 April and 11-24 May

TABLE 2. SENSORS AND DATA RECORDERS

INSTRUMENT	COMPANY	LOCATION	MODEL
Shortwave radiation			
Downward	Eppley Laboratory	Newport, RI	8-48
Reflected	Eppley Laboratory	Newport, RI	PSP
Net all-wave radiation	REBS	Seattle, WA	Q*6
Soil heat conduction	REBS	Seattle, WA	HFT-1
Canopy temperature	Everest Interscience	Fullerton, CA	4000ALCS
Air temperature/Relative humidity	Vaisala	Helsinki, Finland	HMD30UYB
Rainfall	Campbell Sceintific	Logan, UT	TE525
Data loggers	Licor	Lincoln, NE	LI-1000
Porometer	Delta-T	Cambridge, England	AP4
Photosynthetically active radiation (PAR)	Decagon	Pullman, WA	Quantum sensor
Below-canopy PAR	Decagon	Pullman, WA	CEP

Note: RI: Rhode Island; WA: Washington; CA: California; UT: Utah; NE: Nebraska.

the first several weeks of the rainy season, beginning in May. Rainfall measurements continued until August. Characteristics of each measurement site are given in Table 3. Figures 1 and 2 provide maps showing the locations of measurement sites. The Brazil site referred to as "Slashed vegetation" was a field where 7-year secondary vegetation had recently been cut. The slashed vegetation remained on the ground at the time of the observations. Later, after the vegetation had dried for several weeks, the field was burned. Measurements at the same site after the burn are listed under "Burned slash". Table 4 gives the mean vegetation height and sensor heights at each site. Because land cover patches are small in the two study areas, upwind fetch at some sites was less than optimal. We placed the instruments as close as possible to the canopy (or ground in the case of bare soil) in order to minimise fetch-related errors, but not so low as to be affected by individual obstacles. We believe fetch distances at our sites to be adequate under the very low wind speed conditions experienced throughout most of the observation periods.

Energy partitioning

Net radiation, i.e. radiant energy absorbed minus that emitted, is partitioned into sensible and latent energy fluxes to the atmosphere and changes in sensible energy storage in the above-ground biomass and the soil. Neglecting energy storage in the above-ground biomass, we can represent the surface energy balance with the simple expression:

$$R_n = \lambda E + H + G \quad (1)$$

where R_n = net radiation [W m^{-2}], λ = latent heat of vaporization [28.36 W m^{-2} (mm d^{-1})$^{-1}$], E = evaporation [mm d^{-1}], G = soil heat conduction defined as positive downwards [W m^{-2}], and H = sensible energy flux [W m^{-2}]. H can be estimated as (Monteith, 1973):

$$H = \frac{\rho C_p (T_c - T_a)}{r_{ac}} \quad (2)$$

where ρ = the air density [kg m^{-3}], C_p = specific heat of air at constant pressure [J kg^{-1} K^{-1}], T_c = canopy temperature [K] T_a = air temperature [K], and r_{ac} = stability corrected aerodynamic resistance [s m^{-1}]. For neutral stability, aerodynamic resistance to water vapour diffusion [s m^{-1}] can be estimated as (Brutsaert & Stricker, 1979):

$$r_a = \frac{\ln\left(\frac{z_a - d}{z_0}\right)\ln\left(\frac{z_a - d}{z_{0h}}\right)}{k^2 u} \quad (3)$$

where z_o = roughness length for momentum transfer [m], z_{0h} = roughness length for sensible and latent heat transfer [m], z_a = wind measurement height [m], and d = zero plane displacement height [m], k = von Karman constant (0.41), and u = wind velocity. For non-neutral conditions, corrections suggested by Pruitt *et al*. (1973) are applied.

Roughness length for momentum transfer (z_0) in Equation 3 can be estimated using wind profile measurements:

$$z_0 = \exp\left[\frac{[u_2 \ln(z_{u1} - d) - u_1 \ln(z_{u2} - d)]}{u_2 - u_1}\right] \quad (4)$$

where u_1 and u_2 = wind velocities [m s^{-1}] at heights [m] z_{u1} and z_{u2}. We used Equation 4 to estimate aerodynamic parameters z_0 for the five sites with wind measurements at two or more levels. Only data from periods of neutral stability (Richardson Number between + 0.01; see Oke (1987:380-83)) were used in the analysis. Those results were found to conform very well to the empirical relationships between z_0 and vegetation height *(h)*. Equations given by Rosenberg *et al*. (1983) were used to estimate z_0 and d at other sites as a function of h or the estimated height of roughness elements for bare soil.

The relationship between roughness length for sensible and latent heat transfer (z_{0h}) and z_0 may be approximated as:

$$\ln\frac{z_0}{z_{0h}} = B^{-1} \quad (5)$$

where the parameter B^{-1} depends on the characteristics of the vegetation. Brutsaert (1982:105) summarises experimental results that suggest values of B^{-1} for several vegetation types. We set B^{-1} = 2.3 for all sites.

TABLE 3. SITE CHARACTERISTICS

SITE	ELEVATION (m)	SLOPE (°)	ASPECT (°)	ALBEDO[a]	REPRESENTATIVE SPECIES[b]
Igarapé-Açu, Brazil					
(a) Slashed vegetation	39	0	-	0.142	No live vegetation
(b) Burned slash	30	0	-	0.097	No live vegetation
(c) Bare soil	39	0	-	0.170	*Phaseolus sp. (very sparse)*
(d) Mature cassava	39	0	-	0.176	*Manhiot esceulenta Crantz.; Phenakospermum guyanensis Endl.*
(e) Unused pasture	39	0	-	0.175	Piculho (local name for grass species)
(f) ½ yr Secondary vegetation	39	0	-	0.173	*Phenakospermum; Lacistema pubescens Mart.*
(g) 1-yr Secondary vegetation	39	0	-	0.161	*Cassia riparia HBK; Spermacoce verticillata L. (Borreria verticillata)*
(h) 1-yr Secondary vegetation	30	0	-	0.157	*Lacistema pubescens Mart.; Myrcea bracteata*
(i) 2-yr Secondary vegetation	39	0	-	0.162	*Banara guianensis Aubl.; Lacistema pubescens Mart.; Myrcea bracteata DC*
(j) 2-yr Secondary vegetation	39	0	-	0.172	*Banara guianensis Aubl.; Lacistema pubescens Mart.; Myrcea bracteata DC*
(k) 10-yr Secondary vegetation	39	0	-	0.135	*Phenakospermum guyanensis Endl.*
Pang Khum, Thailand					
(l) Harvested barley	1,240	17	65	0.164	No live vegetation
(m) Fallow rice paddy	1,120	0	-	0.141	*Fimbristylis aestivalis (Retz.) Vahl. var. aestivalis (Cyperaceae)* *Digitaria seigera Roth ex Roem. & Schult. var. setigera (Gramineae)*
(n) Irrigated bare soil	1,120	9	270	0.085	No live vegetation
(o) 2-yr Secondary vegetation	1,220	18	35	0.132	Shrub dominated *Ageratina adenophorum (Spreng.) R. King and H. Robinson (Compositae)* *Digitaria seigera Roth ex Roem. & Schult. var. setigera (Gramineae)*
(p) 3-yr Secondary vegetation	1,170	3	75	0.171	Grass dominated *Imperata cylindrica (L.) P. Beauv. var. major (Nees)* C.E. Hubb. ex Hubb. & Vaugh. (Gramineae)
(q) 8-yr Secondary vegetation	1,290	21	300	0.115	*Lithocarpus elegans (Bl.) Hatus. ex Soep. (Fagaceae)* *Gluta tavoyana Wall. ex Hk. f. (Anacardiaceae)*
(r) 25-yr Secondary vegetation	1,240	14	310	0.134	*Lithocarpus elegans (Bl.) Hatus. ex Soep. (Fagaceae)* *Gluta tavoyana Wall. ex Hk. f. (Anacardiaceae)*

[a]Giambelluca (1996).
[b]Based on a survey conducted by plant taxonomist J.F. Maxwell (1993, personal communication) who was at that time a member of the Faculty of Biology and Head of the herbarium at Chiang Mai University.

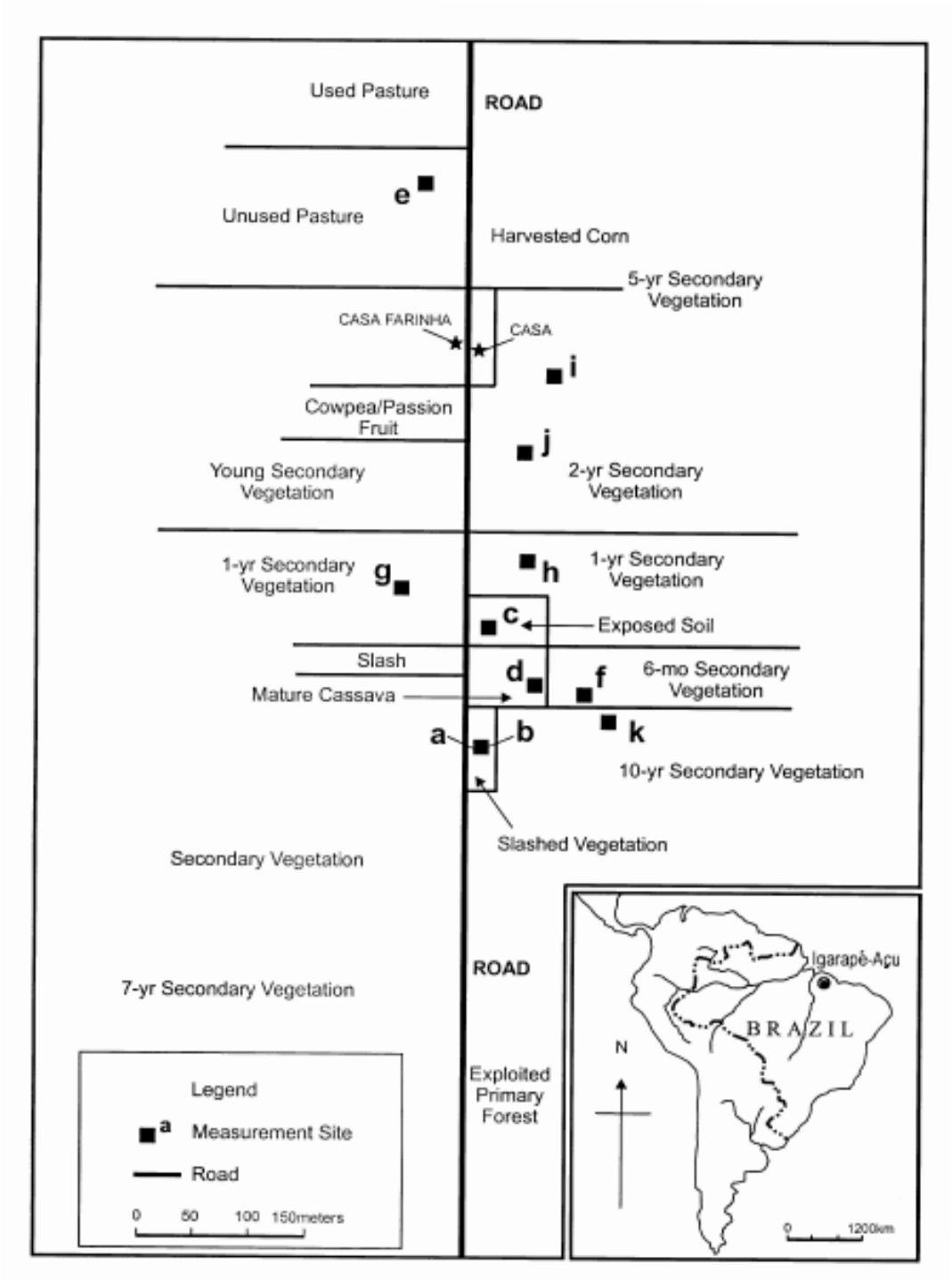

Figure 1. Sites of meteorological measurements at Igarapé Açu, Pará, Brazil.

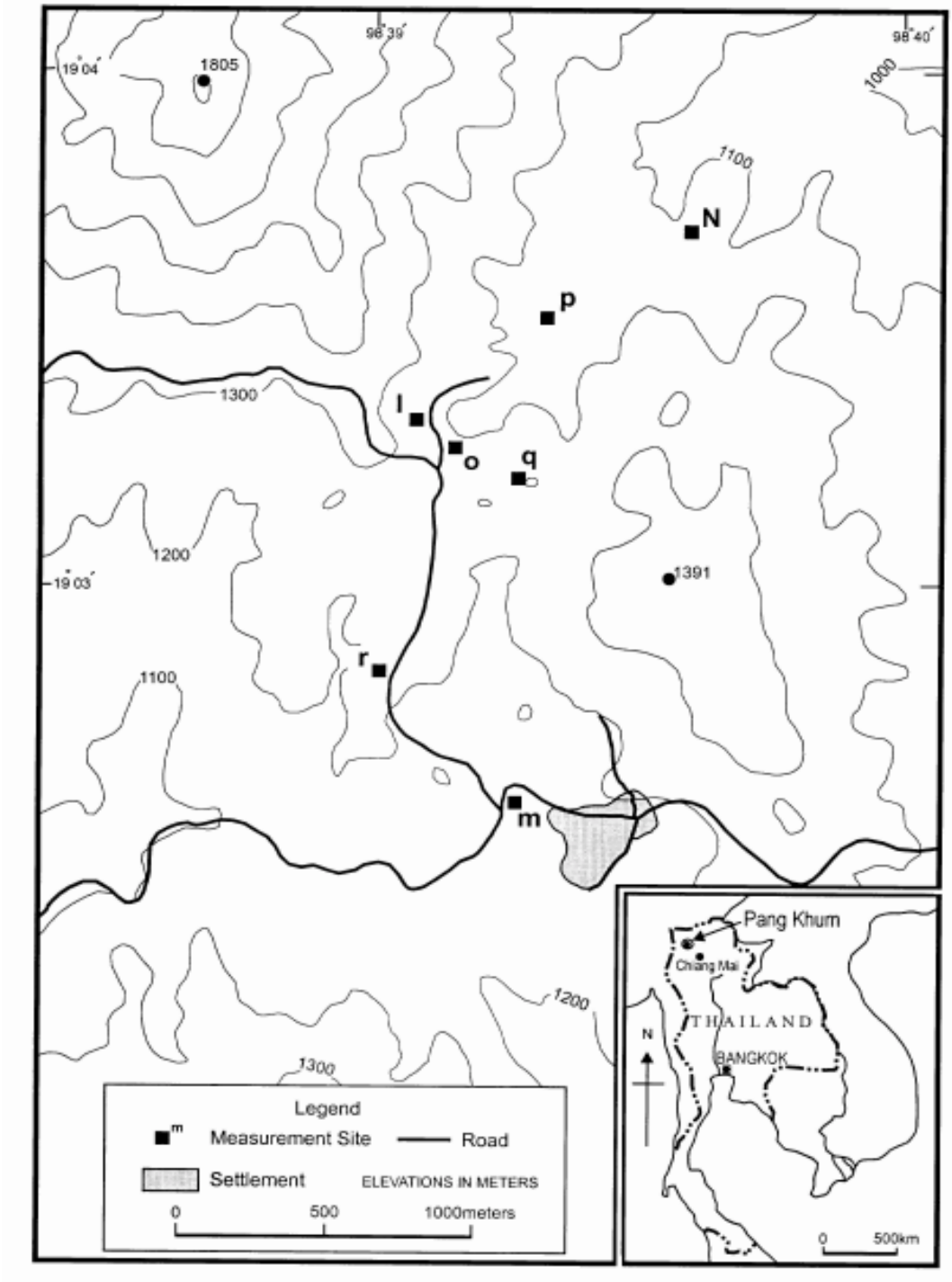

Figure 2. Sites of meteorological measurements at Pang Khum, Chiang Mai, Thailand.

TABLE 4. MEAN VEGETATION HEIGHT (m) AND SENSOR HEIGHTS (m) AT EACH SITE

SITE	VEG. HT.	z_{rad}[a]	z_{u1}	z_{u2}	z_{u3}	$z_{T/RH1}$	$z_{T/RH2}$	$z_{T/RH3}$
Igarapé-Açu, Brazil								
SHIFT Project Tower[b]	1.8	-	2.3	3.2	6.8	-	-	-
(a) Slashed vegetation	1.3	2.8	-	-	-	2.8	-	-
(b) Burned slash	0.0	2.8	-	-	-	2.8	-	-
(c) Bare soil	0.3	2.8	-	-	-	2.8	-	-
(d) Mature cassava	1.4	2.8	-	-	-	2.8	-	-
(e) Unused pasture	0.7	2.8	-	-	-	2.8	-	-
(f) ½ yr Secondary vegetation	0.4	2.8	-	-	-	2.8	-	-
(g) 1-yr Secondary vegetation	0.3	2.8	-	-	-	2.8	-	-
(h) 1-yr Secondary vegetation	1.6	2.8	-	-	-	2.8	-	-
(i) 2-yr Secondary vegetation	1.8	2.8	-	-	-	2.8	-	-
(j) 2-yr Secondary vegetation	1.8	2.8	-	-	-	2.8	-	-
(k) 10-yr Secondary vegetation	4.8	6.0	-	-	-	6.0	-	-
Pang Khum, *Thailand*								
(l) Harvested barley	0.3	4.1	2.9	5.2	-	2.5	4.8	-
(m) Fallow rice paddy	0.0	3.6	1.1	2.6	4.6	0.7	2.2	4.2
(n) Irrigated bare soil	0.0	4.0	1.1	2.8	5.2	0.7	2.4	4.8
(o) 2-yr Secondary vegetation	1.9	5.4	4.2	6.5	-	3.8	6.0	-
(p) 3-yr Secondary vegetation	1.7	5.7	2.9	4.5	6.6	2.4	4.1	6.6
(q) 8-yr Secondary vegetation	3.2	9.3	7.9	10.3	-	7.5	9.9	-
(r) 25-yr Secondary vegetation	5.6	13.1	10.3	11.9	14.4	9.8	11.5	14.0

[a] Sensor heights, z_{rad}, z_u, and $z_{T/RH}$ refer to the height of radiation, wind velocity, and air temperature/humidity sensors, respectively.

[b] Wind measurements taken at the SHIFT project tower located near site (i) were used to estimate wind speed at Brazil sites.

Sugita and Brutsaert (1996) showed that when canopy temperature is measured with a nadir-pointing infrared thermometer, z_{0h} is strongly dependent on sun angle, because of temperature differences among different layers of the canopy. However, this dependence is minimised by pointing the sensor obliquely to properly weight the temperature of the upper layers of the canopy; they suggest an angle of 60º from nadir. In our field observations, done prior to the Sugita and Brutsaert (1996) paper, the sensor was pointed at an angle of approximately 45º from nadir, toward the north, in order to reduce error associated with reflected solar radiation. This angle also gives an estimate of canopy temperature such that z_{0h} is close to that for an isothermal canopy, with only a minimal dependence on sun angle (Sugita &Brutsaert,1996). We did not adjust z_{0h} for sun angle in our calculations.

Using measurements of R_n, G, T_c, estimates of d (based on vegetation height), and vertical profiles of T_a and u, we estimated sensible heat flux *(H)* using Equation 2 and latent energy flux (evaporation) by rearranging Equation 1 as:

$$\lambda E = R_n - G - H \tag{6}$$

Estimation of latent energy flux as a residual (Equation 6) means that errors in measurement of R_n and G, and estimate of H will accumulate in λE. More precise estimation of turbulent energy flux components is possible using other techniques, such as eddy correlation or Bowen ratio. We have found the energy balance approach used here to be highly correlated with Bowen ratio estimates (r^2 = 0.85 for hourly measurements). The instrumentation required is much less expensive and more easily moved from site to site than, for example, a Bowen ratio set up. Energy flux estimates here have greater uncertainty than those based on these other techniques. However, we believe the results are sufficiently accurate to permit comparison among different land covers.

Canopy resistance

Stomatal resistance varies temporally in response to changes in light, leaf temperature, leaf water potential, vapour pressure deficit and water availability in the root zone. When the rate of plant water loss is higher than the rate of intake, plants experience increasing water stress and stomata close partially or completely, thereby increasing stomatal resistance. Stomatal response to water stress is dependent on species physiology and the history of plant water availability which changes throughout a life cycle. Canopy resistance is a variable describing the aggregated effect of stomatal resistance on the evaporation rate of the stand. The role of canopy resistance in regulating evaporation from a vegetated surface is described by the Penman-Monteith equation (Monteith, 1965):

$$\lambda E = \frac{\Delta(R_n - G) + \dfrac{\rho C_p}{r_a}(e_s - e)}{\Delta + \gamma\left(\dfrac{r_a + r_c}{r_a}\right)} \tag{7}$$

where Δ = the slope of the saturation vapour pressure versus temperature curve [mb K^{-1}], e_s = the saturation vapour pressure [mb], e = the ambient vapour pressure [mb], γ = the psychrometric constant [mb K^{-1}], and r_c = the canopy resistance [s m^{-1}].

To estimate canopy resistance, we took stomatal resistance measurements at three sites in Thailand (3-, 8- and 25-year secondary vegetation); in total, 221, 178 and 443 stomatal resistance samples were taken respectively at these three sites. Measurements were taken for a variety of representative species, at different levels within the canopy, over the course of one or more diurnal cycles at each site. Sampling was done between late March and early May, prior to the onset of heavy rainfall. Samples were taken for five, six and eight species respectively at the three sites, and at three or more vertical levels within the canopy of each plant.

Canopy resistance can be calculated as the aggregate of stomatal resistances of all species

at a given site. Because leaves in the upper part of the canopy are more exposed to net radiation, they exert a disproportionately great influence on the overall transpiration rate. Hence, in computing canopy resistance, greater weight should be given to stomatal resistance in more exposed parts of the canopy. In this study, we estimated canopy resistance at the three Pang Khum sites by weighting leaf stomatal resistance measurements according to the leaf area and relative net radiation in each layer as:

$$r_c = \frac{1}{\frac{1}{\overline{r_{s1}}/LAI_1} + \frac{R_{n1}/R_{n2}}{\overline{r_{s2}}/LAI_2} + \cdots + \frac{R_{n1}/R_{ni}}{\overline{r_{si}}/LAI_i}} \qquad (8)$$

where r_c = canopy resistance, $\overline{r_s}$ = average stomatal resistance, LAI = leaf area index (ratio of leaf area to projected ground area), R_n = net radiation, and the subscripts 1, 2 and i refer to the uppermost, second and ith layers of vegetation respectively. Light extinction was used to estimate the leaf area above the ceptometer. We estimated LAI at various levels within the canopy (corresponding to the layers in which stomatal resistance measurements were taken) at each site. Estimates were derived from measurements of canopy light extinction using the relationship suggested by the ceptometer operator's manual (Decagon Devices, 1993).

RESULTS AND DISCUSSION

Diurnal patterns

In Figure 3, the mean diurnal cycles of energy flux components are shown for each site. In general, the individual flux components at each site follow the diurnal pattern of net radiation. For sites where this is not the case, brief explanations follow. For slashed vegetation (a), evaporation is high in the morning when the surface is wetted with dew, then ceases by noon. Negative values in the afternoon are spurious and probably result from excluding sensible heat storage in the biomass. For the burned slash site (b), evaporation is very low throughout the diurnal cycle, confirming that the ash-covered soil surface is very dry immediately following the burn. Observations at the bare soil site (c) were taken during 7-9 November 1992. Small rainfall events, sufficient to wet the soil surface, were recorded on November 7 and 8. High evaporation in the morning results from high moisture availability of the wet soil; evaporation is reduced later in the day after the surface has dried. The evaporation pattern of the mature cassava site (d) suggests strong stomatal control under moisture stress conditions. Observations for site (f) were taken in the same field as site (d), but about 1 week later. During that time, the cassava had been harvested, exposing the young (approximately 0.5 year) secondary vegetation that was previously the understory. No significant rainfall occurred in the interim and weather conditions were otherwise similar. Note that evaporation is generally higher and the midday depression less conspicuous for the newly exposed secondary vegetation in comparison with the cassava. Contrast this with the harvested barley site (l) in Pang Khum, where no live vegetation remained after harvest. There, evaporation rates were extremely low and sensible heat flux correspondingly high throughout the day. Among the other Pang Khum sites, only the 2-year secondary vegetation site (o) has an unusual diurnal pattern. The erratic fluxes there may be the result of brief, intense rainfall events which occurred during the afternoons of three out of six observation days.

Mean energy partitioning

Because observations over different land covers were not made simultaneously, day-to-day atmospheric variation and differences due to geographical separation of the eastern Amazon and northern Thailand in solar angle, cloud cover, precipitable water and atmospheric turbidity affected the measurements over each landcover differently. Under these circumstances, direct comparison among sites of energy fluxes can be done only by examining them in relation to the

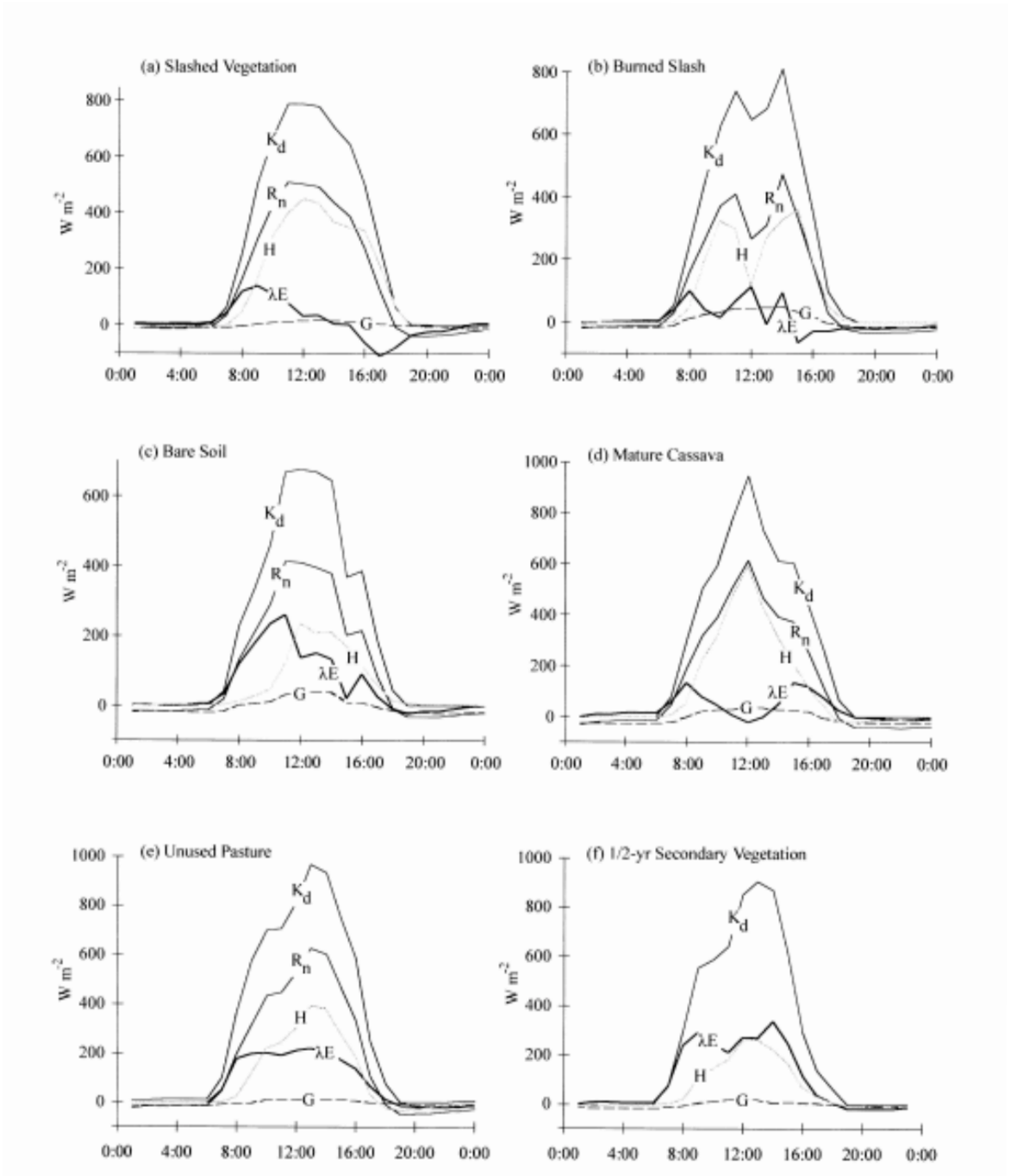

Figure 3. Mean diurnal energy exchange patterns for post-deforestation sites in Igarapé-Açu, Pará, Brazil, and Pang Khum (a-l), Chiang Mai, Thailand (m-r).
K_d = *downward shortwave radiation;* R_n = *net radiation;* λE = *latent heat flux;*
H = *sensible heat flux;* **G** = *soil heat flux.* R_n *was not measured at site (f).*

(Continued overleaf)

Figure 3 (continued)

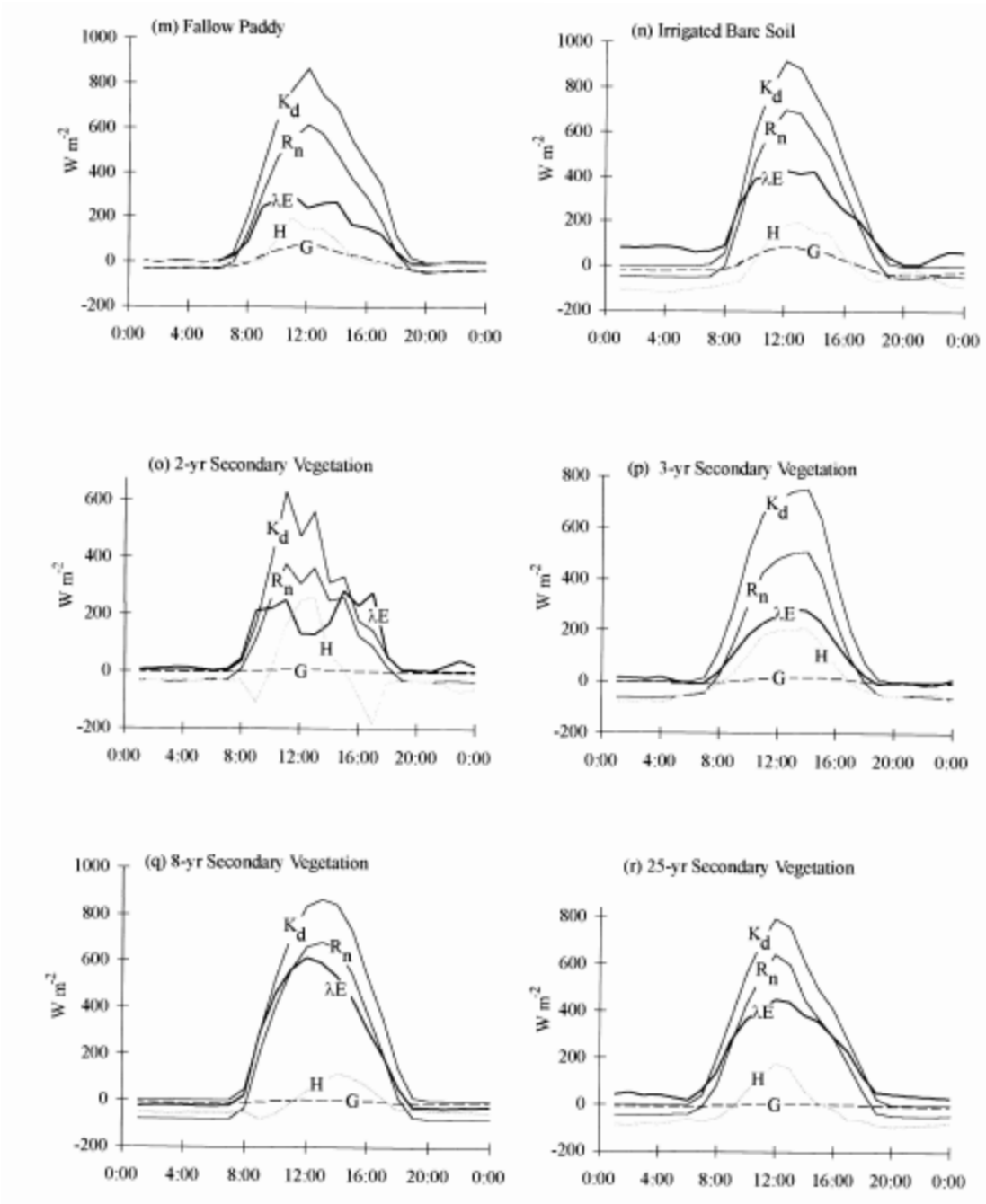

Figure 3 (continued)

corresponding incoming solar radiation, or in terms of the fraction of net radiation.

Field data show that recently disturbed sites are very different in terms of energy partitioning than deforested landscapes that have matured over time since disturbance (Table 5). For example, soil heat flux *(G)* during the daytime accounts for a much lower fraction of net radiation for advancing secondary vegetation sites than for more recently disturbed sites. This effect is clearly seen in the contrast in daytime *G* values for agricultural versus secondary vegetation sites in Thailand.

Results clearly distinguish among land covers on the basis of *E* versus *H* partitioning. Agricultural sites can be classified into three groups: slash and burn sites, non-irrigated swidden sites, and irrigated sites (Figure 4a). Not surprisingly, the evaporative fraction $(\lambda E/R_n)$ is extremely low (and hence the sensible heat fraction large) for slash and burned slash. Evaporative fractions were moderately low for non-irrigated swidden sites and high for irrigated sites. Secondary vegetation sites can also be placed into three groups on the basis of age: 0-1 year, 2-3 years and 8-25 years (Figure 4b). These observations verify that the evaporative fraction of secondary vegetation is low initially, but increases rapidly with age.

Comparison with other forested and deforested sites

Numerous other field studies have been done of energy flux over tropical forest and pasture. Table 6 shows the evaporation estimates of some of those studies in comparison with our estimates. For tropical rainforest, average annual λE is typically around 100-110 W m^{-2}, with $\lambda E/R_n$ of up to

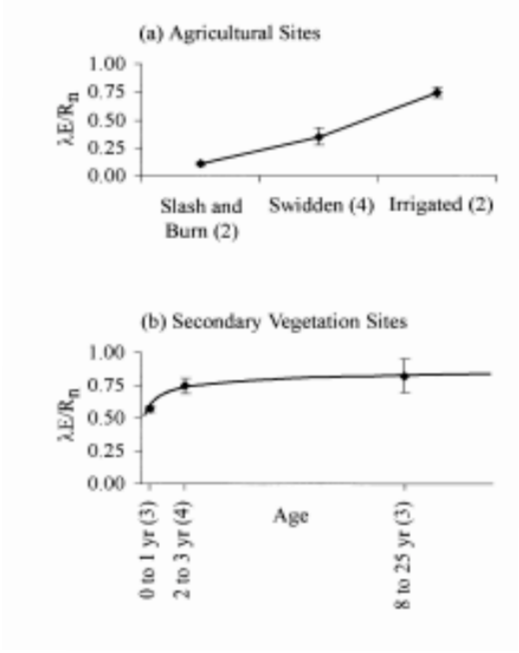

Figure 4. Mean evaporative fractions ($\lambda E/R_n$) for (a) agricultural, and (b) secondary vegetation sites in Igarapé-Açu, Pará, Brazil, and Pang Khum, Chiang Mai, Thailand. Vertical bars show + 0.5 standard deviations about the mean. Sample size for each category is shown in parentheses next to the axis label.

TABLE 5. MEAN ENERGY FLUXES

SITE	K_d[a] (W m^{-2})		R_n (W m^{-2})		G (W m^{-2})		G/R_n		λE (W m^{-2})		$\lambda E/R_n$		H (W m^{-2})		H/R_n	
	Day[b]	All	Day	All	Day	All	Day	All	Day	All	Day	All	Day	All	Day	All
Igarapé-Açu, Brazil																
(a) Slashed vegetation	463	251	272	137	7	0	0.03	0.00	25	11	0.09	0.08	240	126	0.88	0.92
(b) Burned slash	409	221	216	106	21	5	0.10	0.05	26	10	0.12	0.09	169	91	0.78	0.86
(c) Bare soil	361	195	208	102	9	-3	0.04	-0.03	106	55	0.51	0.54	93	50	0.45	0.49
(d) Mature cassava	453	245	278	136	12	-4	0.04	-0.03	54	29	0.19	0.21	212	111	0.76	0.82
(e) Unused pasture	526	288	313	157	5	-1	0.02	-0.01	142	73	0.45	0.46	166	85	0.53	0.54
(f) 1/2 yr secondary vegetation	453	245	300[c]	156[c]	5	2	0.02	0.01	182	95	0.61	0.61	113	59	0.38	0.38
(g) 1-yr secondary vegetation	452	245	268	128	26	3	0.10	0.02	140	71	0.52	0.55	102	54	0.38	0.42
(h) 1-yr secondary vegetation	489	264	308	154	8	2	0.03	0.01	180	88	0.58	0.57	120	64	0.39	0.42
(i) 2-yr secondary vegetation	397	218	243	114	2	-4	0.01	-0.04	167	88	0.69	0.77	74	30	0.30	0.26
(j) 2-yr secondary vegetation	409	225	238	119	2	-5	0.01	-0.04	189	103	0.79	0.87	47	21	0.20	0.18
(k) 10-yr secondary vegetation	422	228	273	134	2	0	0.01	0.00	145	75	0.53	0.56	126	59	0.46	0.44
Pang Khum, Thailand																
(l) Harvested barley	457	248	279	123	18	6	0.06	0.05	68	21	0.24	0.17	193	96	0.69	0.78
(m) Fallow rice paddy	450	245	254	124	27	1	0.11	0.01	171	93	0.67	0.75	56	30	0.22	0.24
(n) Irrigated bare soil	448	243	330	158	31	5	0.09	0.03	266	171	0.81	1.08	33	-18	0.10	-0.11
(o) 2-yr secondary vegetation	252	137	176	82	2	0	0.01	0.00	155	90	0.88	1.10	19	-8	0.11	-0.10
(p) 3-yr secondary vegetation	392	213	233	98	10	4	0.04	0.04	144	80	0.62	0.82	79	14	0.34	0.14
(q) 8-yr secondary vegetation	454	246	320	137	0	-3	0.00	-0.02	313	158	0.98	1.15	7	-18	0.02	-0.13
(r) 25-yr secondary vegetation	413	225	285	141	2	0	0.01	0.00	274	168	0.96	1.19	9	-27	0.03	-0.19

[a]K_d = downward shortwave radiation; R_n = net radiation; G = soil heat flux (positive downward) λE = latent heat flux; H = sensible heat flux to the atmosphere.

[b]Day refers to 12-hour period 6:00-18:00.

[c]Net radiation at site (f) estimated from solar radiation measurements.

TABLE 6. COMPARISON OF EVAPORATION ESTIMATES FOR VARIOUS TROPICAL SITES [a]

LAND COVER	SITE (SOURCE)	DRY CONDITION		WET CONDITION		ANNUAL MEAN	
		λE (W m^{-2})	$\lambda E/R_n$	λE (W m^{-2})	$\lambda E/R_n$	λE (W m^{-2})	$\lambda E/R_n$
Other Field Studies							
Forested	Tropical lowland forests (Bruijnzeel, 1990)[b]	-	-	-	-	111	-
	Central Amazonian rainforest (Shuttleworth, 1988)[c]	94[d]	0.80	96[e]	1.00	102	0.90
	Central Amazonian rainforest (Roberts *et al*., 1993)[f]	64[g]	-	-	-	-	-
		129[h]	-	-	-		-
		105[i]	-	118[j]		-	-
	Central Thailand tropical forest (Pinker *et al*., 1980)[c]	18[k]	0.13	94[l]	0.69	-	-
Deforested	Amazonian pasture (Wright *et al*., 1992)[m]	60[n]	0.52	108[o]	0.70	-	-
	Two-year secondary SHIFT (Holscher *et al*., 1997)[p]	91[q]	0.57	88[r]	0.75	111	0.80
Results of this study							
Secondary vegetation	0 to 1 year	85	0.57	-	-	-	-
	2 to 3 years	90	0.75	-	-	-	-
	8 to 25 years	143	0.82	-	-	-	-
Agriculture	Slash and burn	11	0.11	-	-	-	-
	Swidden	45	0.35	-	-	-	-
	Irrigated	-	-	132	0.74	-	-

[a] Dry and wet conditions are relative for a given site; for Amazonian sites, in particular, "dry" periods may have received substantial rainfall
[b] Average of water balance-derived estimates from numerous watershed studies
[c] Based on model estimate with measured micrometeorological input
[d] September 1985
[e] February 1984
[f] Based on eddy correlation measurements
[g] September 1983
[h] July/August 1984
[i] July/August 1985
[j] April/May 1985
[k] January 1970
[l] June 1970
[m] Based on profile, eddy correlation, and Bowen ratio measurements
[n] 12-day period during October/November 1990
[o] 10-day period during October 1990
[p] Based on Bowen ratio measurements
[q] September 1992
[r] April 1993

0.90. In contrast, forest in central Thailand showed a marked annual cycle in evaporation associated with monsoon-related changes in moisture availability (Pinker *et al*., 1980); $\lambda E/R_n$ ranged from 0.13 (dry season) to 0.69 (wet season). For Amazonian pasture (Wright *et al*., 1992) and young secondary vegetation (Hölscher *et al*., 1997), $\lambda E/R_n$ was lower than that of forest, particularly during dry periods.

Note that the SHIFT project (Hölscher *et al*., 1997), which used an independently measured Bowen ratio data set for the same Igarapé-Açu study site, estimated evaporation to be 4.5 mm d^{-1}, equivalent to 128 W m^{-2} or $\lambda E/R_n = 0.81$, for October 1992. Sites (i) and (j) were located 11 m and 60 m from the SHIFT meteorological tower, respectively, in the same stand of 2-year secondary vegetation. For 23-26 October at site (i), λE was 88 W m^{-2}, and for 26-28 October at site (j), λE was 103 W m^{-2}. $\lambda E/R_n$ was 0.77 and 0.87, respectively for the two sites. Hölscher *et al*. (1997) estimated the annual evaporation at that site to be 3.9 mm d^{-1} (111 W m^{-2}), or $\lambda E/R_n = 0.80$.

Other studies suggest that for dry season conditions, $\lambda E/R_n$ is about 0.8 for tropical forest and 0.5 for pasture (Table 6). Our results confirm low dry season evaporation rates for recently cleared sites, but indicate that the evaporative fraction begins to increase soon after secondary vegetation is allowed to grow. On average for our secondary vegetation sites in Igarapé-Açu and Pang Khum, $\lambda E/R_n$ had recovered to 0.75 within two to three years. For three older secondary vegetation (8-25 years) we found the evaporative fraction to average 0.82, very close to the forest value, but with some notable variation among sites discussed below.

Among the three advanced secondary vegetation sites, daytime $\lambda E/R_n$ was only 0.53 at the 10-year site at Igarapé-Açu (site k), but was very high (0.96 and 0.98) at the two Pang Khum sites (q and r). This difference may be explained by differences in vegetation type and climate regime. Sá *et al*. (1993) stated that the 10-year site at Igarapé-Açu was not representative of all secondary vegetation sites of this age in the study region because of the exceptional dominance of *Phenakospermum guyanensis*. This species has very large banana-like leaves, which intercept and store rainfall effectively, allowing a relatively low fraction of rain water to reach the soil (Sá *et al*., 1993). As a result of high interception evaporation during rainy periods, this site may have somewhat reduced soil moisture storage at the start of dry periods and exhibit water stress sooner than other sites. Indeed, soil moisture, leaf water potential and stomatal resistance measurements at the site, all indicated greater water stress than at neighboring sites (Sá *et al*., 1993). At the two Pang Khum sites, on the other hand, vegetation was dominated by tree species typical of undisturbed forest, such as *Lithocarpus elegans*, which do not have exceptional rainfall interception characteristics. Regarding the climate regime, Pang Khum normally experiences a six-month period of almost no rainfall; in contrast Igarapé-Açu has a shorter, less intense dry season. At the time of our measurements in Pang Khum, swidden fields (e.g. the harvested barley site) were extremely dry. In the highly fragmented landscape, these patches became sources of sensible heat which was advected to neighboring stands of deeply-rooted trees, which in turn exhibited higher rates of evaporation. Based on these observations, we believe that as long as sufficient soil water is available, dry-season evaporation within patches of advanced secondary vegetation and forest will be very high, even exceeding net radiation (we found $\lambda E/R_n$ of 1.15 and 1.19 for sites q and r). Younger secondary vegetation at Pang Khum, such as site (p), with correspondingly shallower roots, experiences water stress during the dry season and evaporation is reduced by increased stomatal resistance. In the

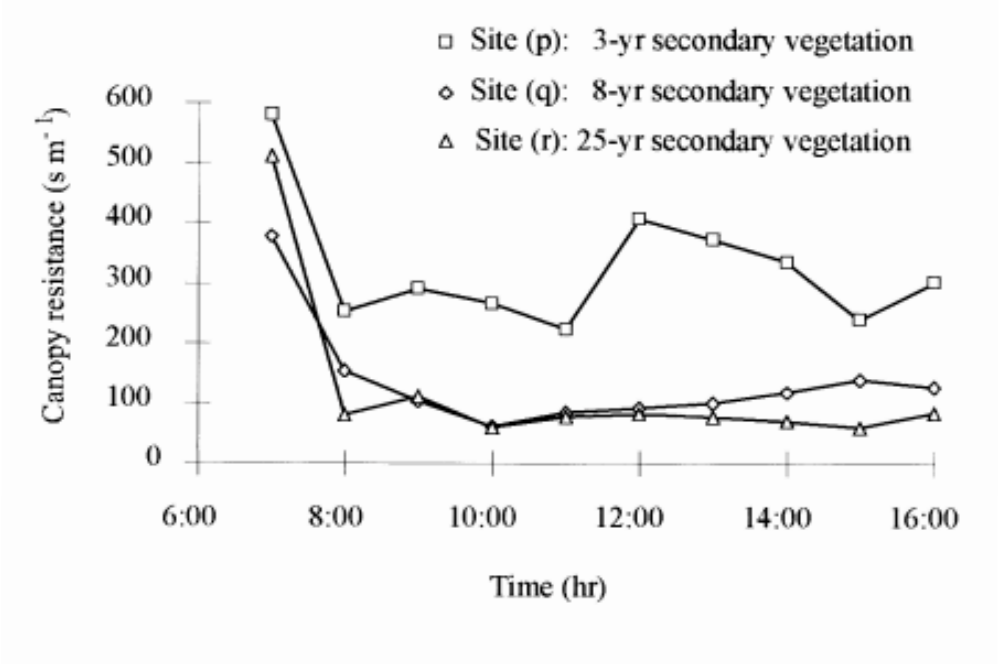

Figure 5. Canopy resistance for a 3-, 8- and a 25-year secondary vegetation site in Pang Khum, Chiang Mai, Thailand.

following section, we give the results of measurements showing higher stomatal resistance in younger secondary vegetation as evidence of the effects of moisture stress.

Canopy resistence

Site-specific canopy resistances calculated from the stomatal resistance and LAI data (Equation 8) are very informative of the influences of different land cover on evapotranspiration. Figure 5 shows that canopy resistances of 8- and 25-year secondary vegetation (sites q and r) are very similar to each other, while that of the 3-year secondary vegetation site (p) is much higher throughout the diurnal cycle. Holding all other variables constant at typical values, the difference in canopy resistance shown implies a reduction in evaporation of about 50 per cent based on the Penman-Monteith model (Equation 7). This is consistent with our energy balance measurements and verifies that evaporation at more mature secondary vegetation sites is significantly higher than that at sites abandoned for only a few years. Minimum canopy resistance was 223, 61, and 58 s m^{-1}, respectively at the 3-, 8- and 25-year sites respectively. In comparison, minimum canopy resistance is typically set at 140 and 32 s m^{-1} (Xue *et al*., 1996), respectively, for grass-covered and forested land, representing the contrasting scenarios in GCM deforestation experiments.

CONCLUSIONS

Regional climatic and hydrologic change has been predicted to result from tropical deforestation due, in part, to large changes in the way absorbed radiant energy is partitioned into latent and sensible heat fluxes to the atmosphere. Specifically, replacement of multi-story forest with lower vegetation is expected to reduce latent energy flux due to lower roughness length, less canopy rainfall interception, and greater canopy resistance during dry periods. In general, our results confirm that evaporation rates for actively or

recently cultivated sites are significantly lower than for forested sites, and rates of sensible energy flux are correspondingly higher. In fact, evaporation rates at those sites, estimated from dry season measurements, are well below annual average values predicted for the uniform grassland scenarios of GCM deforestation simulations. However, for secondary vegetation, evaporation rates are much higher than for actively used sites, even approaching forest values at the most mature sites. In Thailand, 8- and 25-year secondary vegetation sites were found to have very high rates of evaporation, with latent energy flux accounting for 115 and 119 per cent of net radiation respectively. These high ratios are associated with net downward (negative) sensible energy flux, indicating the presence of high positive heat advection at both sites. In the highly patchy landscape of northern Thailand, actively and recently cultivated fields with low dry season evaporation are sources of sensible energy being advected to neighbouring stands of advanced secondary vegetation. As long as the soil moisture reservoir of the more deeply rooted trees of older secondary vegetation patches is adequate, evaporation there will be enhanced. Extrapolating this effect over the region, we can speculate that the negative effects of actively used deforested lands on the areal average evaporation rate are partly offset by enhancement of evaporation in small patches of intermediate and advanced secondary vegetation and forest. Because the influence of advection is confined to areas near land cover boundaries, the regional effect is dependent upon the scale of the land cover units; the effect increases as patches get smaller (Klaassen, 1992). We are currently conducting detailed measurements aimed at quantifying this effect in the fragmented land cover of northern Vietnam.

Using dry season measurements for both the Brazil and northern Thailand study areas, we found evaporation to be lower at actively used sites and higher at secondary vegetation sites than that predicted in model simulations of deforestation. Because of the large areal extent of secondary vegetation in both the Amazon (Moran *et al*., 1994) and northern Thailand (Fox *et al*., 1995), and because of the effects of positive heat advection in areas with highly patchy land covers, we believe that regional evaporation rates in deforested areas of the tropics are likely to be higher than those predicted in some GCM deforestation experiments. This suggests that subsequent deforestation-related impacts on the hydrologic cycle, such as a reduction in rainfall, may not be as severe as those predicted by such simulations.

Energy flux estimates presented here are subject to uncertainty due to the short periods of observation, measurement errors, and errors in setting parameter values. These results should be confirmed with continuous multi-year simultaneous measurements over various land covers, using eddy-correlation, Bowen ratio or other more precise techniques.

The results presented here are not intended to encourage current practices leading to rapid forest loss in the tropics. The continuing effects of deforestation on atmospheric chemistry, loss of plant biodiversity and animal habitat and the destruction of the cultures of forest-dwelling people will remain critical issues, undiminished by any reassessment of direct climate effects.

ACKNOWLEDGMENTS

The research reported here was initiated and carried out with the support and cooperation of numerous individuals associated with the Sam-Mun Highland Development Project; Multiple Cropping Centre, the Geography Department, and the Biology Department at Chiang Mai University; and the East-West Center in Honolulu. We are most grateful to Samer Limchoowong (Sam-Mun Highland Development Project), Methi Ekasingh (Multiple Cropping Centre), Sanay Yarnasarn and Pichayet Onibutr (Geography Department, Chiang Mai), J.F. Maxwell, and Jefferson Fox (East-West Center). We are also deeply

indebted to the people of Pang Khum who gave generously of their knowledge of the land and allowed us to use their land for our measurements. We are especially thankful for the kindness of the Paluk and Nadi Lamer who provided accommodations in Pang Khum as well as advice and assistance at every stage of the field research. Financial support for the field study was provided by the Committee for Research and Exploration, National Geographic Society (grant number 4923-92) and by a University of Hawaii-East-West Center Collaborative Research Grant.

REFERENCES

Bastable, H.G., Shuttleworth, W.J., Dallarosa, R.L.G., Fisch, G. & Nobre, C.A. (1993) 'Observations of climate albedo, and surface radiation over cleared and undisturbed Amazonian forest', *International Journal of Climatology*, 13, 783-96.

Bastos, T.X., Hölscher, D. & Sá, T.D. de A. (1993) 'Climate evaluation in northeast Pará, Igarapé-Açu site', Proceedings, Workshop on Studies on Human Impact on Forest and Floodplains in the Tropics, Belém, 9-12 March, 19.

Bruijnzeel, L.A. (1990) *Hydrology of Moist Tropical Forests and Effects of Conversion: a State of Knowledge Review*, Paris: UNESCO and Amsterdam: Vrije Universiteit.

Bruijnzeel, L.A. (forthcoming) 'Forest hydrology', in J.C. Evans (ed.), *The Forestry Handbook*, Oxford, UK: Blackwell Scientific.

Brutsaert, W. & Stricker, H. (1979) 'An advection-aridity approach to estimate actual regional evapotranspiration', *Water Resources Research*, 15, 443-50.

Brutsaert, W. (1982) *Evaporation into the Atmosphere: Theory, History, and Application*, Dordrecht: D. Reidel, 299.

Culf, A.D., Fisch, G. & Hodnett, M.G. (1995) 'The albedo of Amazonian forest and ranchland', *Journal of Climate*, 8, 1544-554.

Decagon Devices, Inc. (1993) *Sunfleck PAR Ceptometer Operator's Manual*, Pullman, Western Australia: Decagon Devices, Inc.

Eltahir, E.A.B. & Bras, R.L. (1996) 'Precipitation recycling', *Reviews of Geophysics*, 34, 367-78.

Fox, J., Kanter, R., Yarnasarn, S., Ekasingh, M. & Jones, R. (1994) 'Farmer decision making and spatial variables in Northern Thailand', *Environmental Management*, 18, 391-99.

Fox, J., Krummel, J., Yarnasarn, S., Ekasingh, M. & Podger, N. (1995) 'Land use and landscape dynamics in Northern Thailand: Assessing change in three upland watersheds', *Ambio*, 24, 328-34.

Giambelluca, T.W. (1996) 'Tropical land cover change: Characterizing the post-forest land surface', in T.W. Giambelluca & A. Henderson-Sellers (eds.), *Climate Change: Developing Southern Hemisphere Perspectives*, Chichester: John Wiley and Sons, 293-318.

Giambelluca, T.W., Tran, L.T., Ziegler, A.D., Menard, T.P. & Nullet, M.A. (1996) 'Soil-vegetation-atmosphere processes: Simulation and field measurement for deforested sites in northern Thailand', *Journal of Geophysical Research*, 101, 25, 867-885.

Giambelluca, T.W., Hölscher, D., Bastos, T.X., Frazão, R.R., Nullet, M.A. & Ziegler, A.D. (1997) 'Observations of albedo and radation balance over post-forest land surfaces in eastern Amazon Basin', *Journal of Climate*, 10, 919-28.

Giambelluca, T.W., Fox, J., Yarnasarn, S., Onibutr, P. & Nullet, M.A. (1999) 'Dry-season radiation balance of land covers replacing forest in northern Thailand', *Agricultural and Forest Meteorology*, 95, 53-65.

Hansen, P.K. (1992) *An Account of the Forest in a Watershed Area in Northern Thailand*,

Department of Economics and Natural Resources, Copenhagen, Denmark: Unit of Forestry, Royal Veterinary and Agricultural University.

Henderson-Sellers, A., Zhang, H. & Howe, W. (1996) 'Human and physical aspects of tropical deforestation', in T.W. Giambelluca & A. Henderson-Sellers (eds.), *Climate change: Developing Southern Hemisphere Perspectives*, Chichester: John Wiley and Sons, 259-92.

Hölscher, D., de A. Sá, T.D., Bastos, T.X., Denich, M. & Fölster, H. (1997) 'Evaporation from young secondary vegetation in eastern Amazonia', *Journal of Hydrology*, 193, 293-305.

Jipp, P.H., Nepstad, D.C., Cassel, D.K. & Reis de Carvalho, C. (1998) 'Deep soil moisture storage and transpiration in forests and pastures of seasonally-dry Amazonia', *Climatic Change*, 39, 395-412.

Kato, M. do S.A. & Denich, M. (1993) 'The municipality of Igarapé-Açu-Pará study site', Proceedings, Workshop on Studies on Human Impact on Forest and Floodplains in the Tropics, Belém, 9-12 March, 7-9.

Klaassen, W. (1992) 'Average fluxes from heterogeneous vegetated regions', *Boundary-Layer Meteorology*, 58, 329-54.

McGuffie, K., Henderson-Sellers, A., Zhang, H., Durbridge, T.B. & Pitman, A.J. (1995) 'Global sensitivity to tropical deforestation', *Global Planetary Change*, 10, 97-128.

Monteith, J.L. (1965) 'Evaporation and environment', in *The State and Movement of Water in Living Organisms*, Symposium of Social and Experimental Biology, 19, 205-34.

Monteith, J.L. (1973) *Principles of Environmental Physics*, New York: American Elsevier.

Moran, E.F., Brondizio, E., Mausel, P. & Wu, Y. (1994) 'Integrating Amazonian vegetation, land-use, and satellite data', *BioScience*, 44, 329-38.

Nobre, C.A., Sellers, P.J. & Shukla, J. (1991) 'Amazonian deforestation and regional climate change', *Journal of Climate*, 4, 957-88.

Oke, T.R. (1987) *Boundary Layer Climates*, Second Edition, London: Methuen.

Pinker, R.T., Thompson, O.E. & Eck, T.F. (1980) 'The energy balance of a tropical evergreen forest', *Journal of Applied Meteorology*, 19, 1341-349.

Polcher J. & Laval, K. (1994) 'The impact of African and Amazonian deforestation on tropical climate', *Journal of Hydrology*, 155, 389-405.

Pruitt, W.O., Morgan, D.L. & Lourence, F.J. (1973) 'Momentum and mass transfer in the surface boundary layer', *Quarterly Journal of the Royal Meteorological Society*, 99, 370-86.

Roberts, J., Cabral, O.M.R., Fisch, G., Molion, L.C.B., Moore, C.J. & Shuttleworth, W.J. (1993) 'Transpiration from an Amazonian rainforest calculated from stomatal conductance measurements', *Agricultural and Forest Meteorology*, 65, 175-96.

Rosenberg, N.J., Blad, B.L. & Verma, S.B. (1983) *Microclimate, the Biological Environment*, New York: John Wiley and Sons.

Sá, T.D. de A., Hölscher, D., de Carvalho, C.J.R., Giambelluca, T.W. & Bastos, T.X. (1993) 'Micrometeorological and ecophysiological evaluation of secondary vegetation: A step to improve agroforestry systems in the Brazilian eastern Amazon', paper presented at the International Meeting on Geophysiology of Tropical Intercropping, Guadaloupe, French Antilles, 6-10 December.

Shuttleworth, W.J. (1988) 'Evaporation from Amazonian Rainforest', *Proceedings of the Royal Society of London*, B 233: 321-46.

Sugita, M & Brutsaert, W. (1996) 'Optimal measurement strategy for surface temperature to determine sensible heat from anisothermal vegetation', *Water Resource Research*, 32(2), 129-234.

Wright, I.R., Gash, J.H.C., Da Rocha, H.R., Shuttleworth, W.J., Nobre, C.A., Maitelli, G.T., Zamparoni, C.A.G.P. & Carvalho, P.R.A. (1992) 'Dry season micro-meteorology of central Amazonian ranchland', *Quaterly Journal of the Royal Meteorological Society*, 188, 1083-099.

Xue, Y., Bastable, H.G., Dirmeyer, P.A. & Seller, P.J. (1996) 'Sensitivity of simulated surface fluxes to changes in land surface parameterizations – A study using ABRACOS data', *Journal of Applied Meteorology*, 35, 386-400.